



Enhanced Solutal Marangoni Flow Using Ultrasound-Induced Heating for Rapid Digital Microfluidic Mixing

Beomseok Cha[†], Woohyuk Kim[†], Giseong Yoon, Hyunwoo Jeon and Jinsoo Park*

School of Mechanical Engineering, Chonnam National University, Gwangju, South Korea

OPEN ACCESS

Edited by:

Sung Yong Jung,
Chosun University, South Korea

Reviewed by:

Hanwook Park,
Soonchunhyang University, South
Korea

Luca Lanotte,
INRA Centre Bretagne-Normandie,
France

*Correspondence:

Jinsoo Park
jinsoopark@jnu.ac.kr

[†]These authors have contributed
equally to this work and share first
authorship

Specialty section:

This article was submitted to
Soft Matter Physics,
a section of the journal
Frontiers in Physics

Received: 03 July 2021

Accepted: 16 August 2021

Published: 30 August 2021

Citation:

Cha B, Kim W, Yoon G, Jeon H and
Park J (2021) Enhanced Solutal
Marangoni Flow Using Ultrasound-
Induced Heating for Rapid Digital
Microfluidic Mixing.
Front. Phys. 9:735651.
doi: 10.3389/fphy.2021.735651

Digital microfluidics based on sessile droplets has emerged as a promising technology for various applications including biochemical assays, clinical diagnostics, and drug screening. Digital microfluidic platforms provide an isolated microenvironment to prevent cross-contamination and require reduced sample volume. Despite these advantages, the droplet-based technology has the inherent limitation of the quiescent flow conditions at low Reynolds number, which causes mixing samples confined within the droplets to be challenging. Recently, solutal Marangoni flows induced by volatile liquids have been utilized for sessile droplet mixing to address the above-mentioned limitation. The volatile liquid vaporized near a sessile droplet induces a surface tension gradient throughout the droplet interface, leading to vortical flows inside a droplet. This Marangoni flow-based droplet mixing method does not require an external energy source and is easy to operate. However, this passive method requires a comparably long time of a few tens of seconds for complete mixing since it depends on the natural evaporation of the volatile liquid. Here, we propose an improved ultrasound-induced heating method based on a nature-inspired ultrasound-absorbing layer and apply it to enhance solutal Marangoni effect. The heater consists of an interdigital transducer deposited on a piezoelectric substrate and a silver nanowire-polydimethylsiloxane composite as an ultrasound-absorbing layer. When the transducer is electrically actuated, surface acoustic waves are produced and immediately absorbed in the composite layer by viscoelastic wave attenuation. The conversion from acoustic to thermal energy occurs, leading to rapid heating. The heating-mediated enhanced vaporization of a volatile liquid accelerates the solutal Marangoni flows and thus enables mixing high-viscosity droplets, which is unachievable by the passive solutal Marangoni effect. We theoretically and experimentally investigated the enhanced Marangoni flow and confirmed that rapid droplet mixing can be achieved within a few seconds. The proposed heater-embedded sessile droplet mixing platform can be fabricated in small size and easily integrated with other digital microfluidic platforms. Therefore, we expect that the proposed sample mixing method can be utilized for various applications in digital microfluidics and contribute to the advancements in the medical and biochemical fields.

Keywords: digital microfluidics, solutal marangoni flow, ultrasound-induced heating, sessile droplet, droplet mixing

INTRODUCTION

Along with the advancements of continuous flow microfluidics, digital microfluidics based on micro-/nano-liter sessile droplets has attained much attention as a promising technology for its various advantages and broad applicability [1–3]. In digital microfluidic platforms, small-volume sessile droplets allow efficient use of samples, short reaction time, and miniaturization of the engineering system, which reduces manufacturing costs and can be adapted to portable devices [3, 4]. The digital microfluidic platform also provides an isolated microenvironment with a low risk of sample cross-contamination and does not require a photolithography process for microchannels [5, 6]. In digital microfluidic applications, basic unit operations within sessile droplets are required such as mixing, migration, merging, and splitting [7]. Rapid and uniform mixing of the sample inside sessile droplets is essential for various biochemical and medical assays in digital microfluidic platforms [8, 9]. However, the sessile droplet-based microfluidic platform has the inherent limitation of the quiescent flow conditions at low Reynolds number, which results in sample mixing induced by Brownian diffusion [10, 11].

Various digital microfluidic mixing methods have been developed to date. These droplet mixing methods could be characterized into passive and active methods depending on whether they involve external forces. Recently, vapor-mediated solutal Marangoni flows have been utilized for sessile droplet mixing in a passive manner [3, 12, 13]. The solutal Marangoni effect is induced by a surface tension gradient along the droplet interface by localized vapor of a volatile liquid near sessile droplets [14]. The surface tension gradient causes shear stress along the droplet interface and thus symmetric vortical flows inside a droplet, which results in sample mixing inside sessile droplets [3, 15]. The key advantages of this mixing method are its passive operation without any external force fields and easy operation at a low cost. However, the limited Marangoni-induced flow of a few mm/s results in comparably long mixing time of several tens of seconds even under well-defined conditions of low-viscosity water droplets only a few mm away from the volatile liquid source, which strictly limits practical applicability of the method.

Several active droplet mixing techniques based on electrowetting on dielectric (EWOD) [7], bulk acoustic wave (BAW) [16], and surface acoustic wave (SAW) [17] have been proposed to address the above-mentioned limitations of the passive method. In the EWOD method, sessile droplets experience an AC electric field produced by planar electrodes for translocation, merging, and mixing [7]. BAWs can also be used to vibrate the substrate on which sessile droplets are deposited and thus induce internal flows inside the droplets [16]. When SAWs propagating on a piezoelectric substrate interact with liquid droplets, they refract into the droplets in the form of longitudinal waves and produce an acoustic streaming flow, resulting in rapid droplet mixing [17]. These active methods provide rapid droplet mixing in a controllable manner, compared to the passive methods. Nonetheless, they all require direct contact of sessile droplets with the electrodes or

substrates, imposing potential undesirable effects on liquid droplets and suspended samples and limiting their practical applicability.

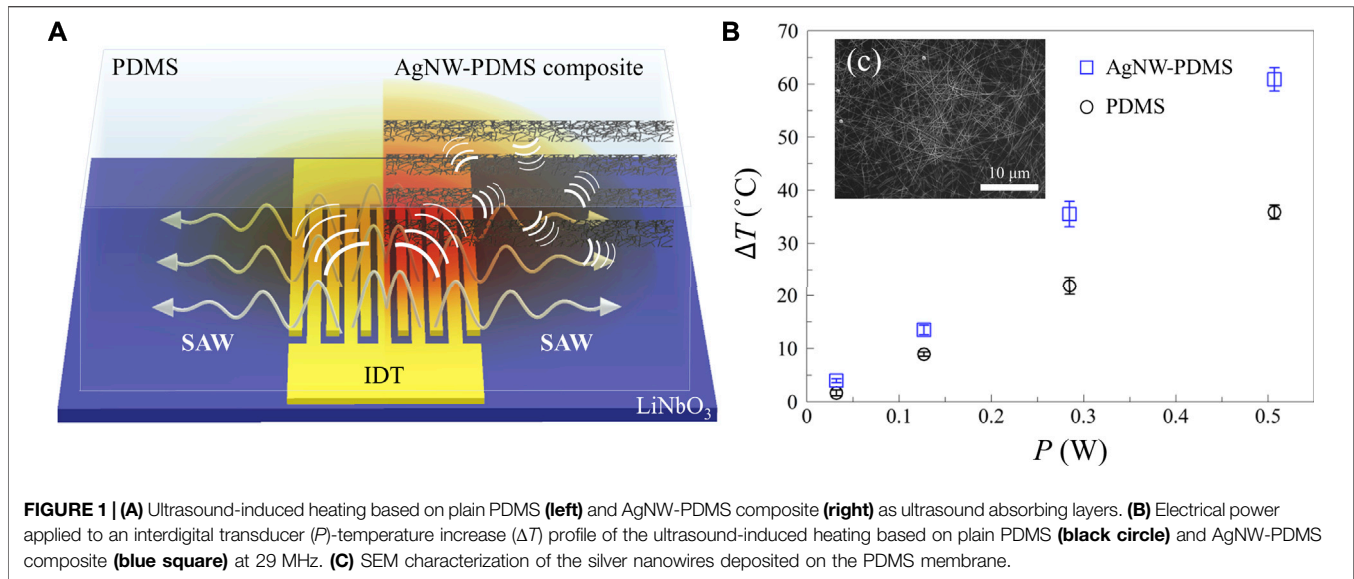
Herein, we propose a rapid digital microfluidic mixing method based on enhanced solutal Marangoni flows using ultrasound-induced heating. The ultrasound-induced heating (UIH) is an energy-efficient micro-heating method that utilizes rapid heat generation by ultrasound absorption in viscoelastic material [18]. We further improved the energy efficiency of the ultrasound-heating method by adopting a nature-inspired ultrasound absorbing fibrous layer which can be seen at moth wings for its survival. The local vapor concentration at the droplet interface is the crucial parameter for the vapor-driven solutal Marangoni effect [3, 12, 13]. The increased temperature accelerates vaporization of the volatile liquid placed near sessile droplets, leading to enhanced vapor-mediated solutal Marangoni flows inside sessile droplets. As a consequence, the time required for uniform sample mixing of the in-droplet sample is dramatically reduced to only a few seconds, and the Marangoni flow velocity is increased up to a few tens of mm/s, compared to the passive solutal Marangoni flow-based method. Also, the proposed heating-mediated Marangoni flow-based mixing method can be applicable to viscous liquid droplets placed relatively far from the volatile liquid. We theoretically and experimentally investigate the proposed digital microfluidic mixing method using particle image velocimetry (PIV) for quantified analysis of the enhanced solutal Marangoni flows. We believe that the proposed digital microfluidic mixing method can be widely utilized for a variety of medical and biochemical assays based on sessile droplets.

METHODOLOGY

Ultrasound-Induced Heating

The UIH is a micro-heating method based on the energy conversion from acoustic energy to thermal energy due to viscoelastic damping of ultrasonic SAWs propagating in a viscoelastic material [19]. As shown in **Figure 1A**, the UIH device is composed of an interdigital transducer (IDT) deposited on a piezoelectric lithium niobate (LiNbO_3) substrate and an ultrasound absorbing layer made of viscoelastic polydimethylsiloxane (PDMS). When an alternating current (AC) signal with the IDT resonant frequency is applied, SAWs are produced from the IDT by the inverse piezoelectric effect and immediately refract into the wave absorbing layer in the form of longitudinal and shear bulk waves. Due to high viscoelastic characteristics of PDMS, the high-frequency mechanical oscillations experience stress-strain hysteresis, causing the wave energy dissipation in the form of heat (thermal energy) [20]. As found in our earlier studies [18, 19, 21, 22] the ultrasound-induced micro-heating method offers rapid, energy-efficient, volumetric heating and 2D spatiotemporal temperature gradient control on the microscale.

In UIH, heat is generated in the viscoelastic layer as the waves are attenuated by viscoelastic damping. In the present study, we further improve the energy efficiency of the UIH by enhancing



ultrasound absorption based on a nature-inspired fibrous network embedded in the ultrasound absorbing layer. Moths are one of the main prey of bats which detect their prey or obstacles using ultrasound. The moth has a hairy structure on its wings to hide from the bat's ultrasound echolocation since the microscale hairs on the moth wings serve as an ultrasound absorber [18, 23]. In analogy to the hairy structure on the moth wing, we have developed an improved UIH method based on a fiber network-embedded viscoelastic wave absorbing layer, as shown in **Figure 1A**. A thin PDMS membrane was first fabricated by spin-coating of uncured PDMS precursor solution, and then silver nanowires (AgNWs) (Flexiowire2040c, SG Flexio) suspended in isopropanol (IPA) were deposited on the oxygen plasma-treated PDMS membrane by air-brushing to form an AgNW-PDMS composite in a layer-by-layer process (**Figure 1C**). The AgNWs have 43 ± 5 nm in diameter and 19 ± 5 μm in length. Due to the acoustic impedance mismatch between PDMS and AgNWs, the AgNW fibrous network in PDMS serve as an ultrasound wave scatterer. As a result, the effective wave attenuation length in PDMS is increased due to random wave scattering, and the amount of heat produced in the wave absorbing layer is increased accordingly. The temperature increase (ΔT) in the UIH device heavily depends on the electrical power (P) applied to the IDT to produce SAWs. We measured the temperature increase in the wave absorbing layers made of plain PDMS and the AgNW-PDMS composite using an infrared thermal camera, as shown in **Figure 1B**. The IDT used in this study had a resonant frequency of 29 MHz for energy-efficient heating [21] and a wave-producing area of 3.1×2.6 mm^2 . For the UIH device, the ultrasound absorbing layer made of the AgNW-PDMS composite was found to have a 61.09% improvement in the temperature increase on average at room temperature of 20°C , compared to that made of plain PDMS. Therefore, we confirmed that the nature-inspired ultrasound-absorbing layer made of the AgNW-PDMS composite can improve the energy efficiency of the conventional UIH method.

Enhanced Solutal Marangoni Effect

In sessile droplet-based microfluidics, the surface tension effect is significant. The Marangoni effect can be induced due to the surface tension gradient along with the droplet interface that can be caused by temperature gradient [19] surfactant [24] or solutes [25]. The vapor-mediated solutal Marangoni effect has been widely studied for translocating [26], splitting [27], and mixing [3] sessile droplets. **Figure 2A** shows a schematic diagram of the vapor-mediated solutal Marangoni effect. A spherical cap-shaped sessile droplet is placed near a capillary tube-based microchannel with one end open toward the droplet. A volatile liquid having a lower surface tension than the sessile droplet liquid, water in this study, flowing in the microchannel is vaporized at the capillary tip and radially diffuses in the direction toward the sessile droplet. As a consequence, the local surface tension gradient is induced along the droplet interface, and this imbalanced surface tension results in Marangoni flows inside of the droplet with a pair of Marangoni vortices. Especially for sessile droplet mixing, the vapor-mediated solutal Marangoni effect has attracted much attention since it can be used to control flows inside sessile droplets without temperature increase and chemical contamination of the droplets.

In the present study, we apply the improved UIH heating to accelerate vaporization of volatile liquid used to induce the enhanced solutal Marangoni effect. From the simplified, steady-state Poisson diffusion equation in the spherical coordinates, assuming that the volatile vapor continuously diffuses in the radial direction with the negligible viscous boundary layer effect, the concentration profile of volatile vapor in the air (c_{air}) can be expressed as [3, 12, 28],

$$c_{air}(x, y) = \frac{1}{2} \frac{c_0 \times (2r_0)}{\sqrt{(d + R - x)^2 + y^2}} \quad (1)$$

where c_0 is the initial concentration at the microchannel, r_0 is the radius of a microchannel, d is the distance between microchannel

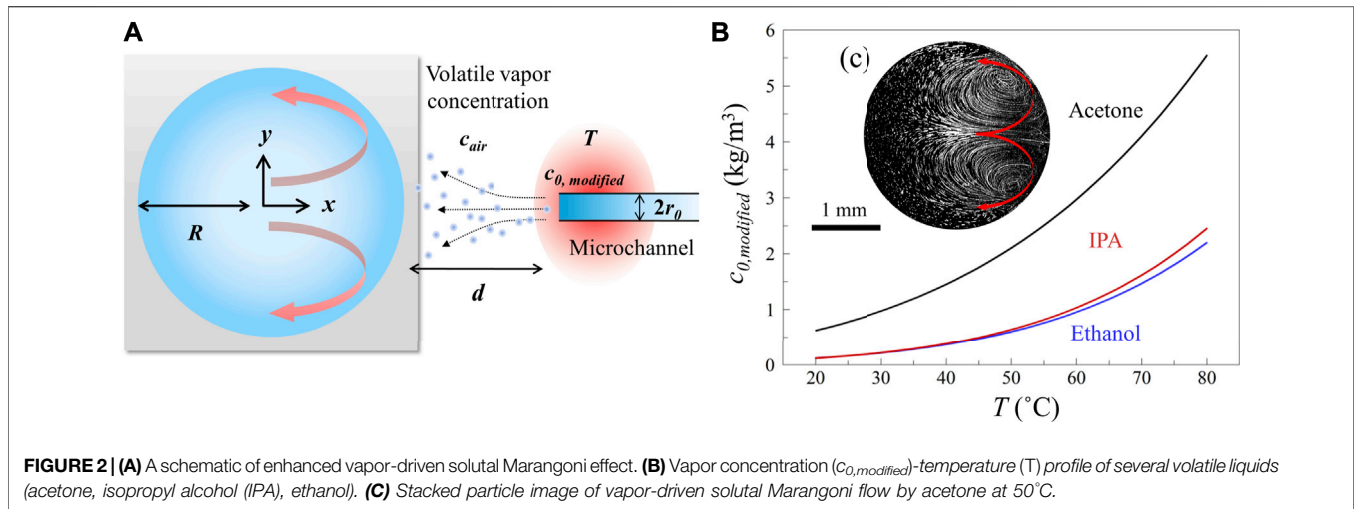


TABLE 1 | Antoine constants and molecular weight of volatile liquids.

	A	B	C	M (g/mol)
Ethanol	8.38235	1739.914	238.131	46.07
Acetone	7.16250	1,225.000	230.000	58.08
IPA	7.74181	1,357.427	197.336	60.10

and sessile droplet, and R is the sessile droplet radius. We placed the volatile liquid on one side of the droplet so that the volatile vapor effect region was defined as $0 < x < R$ and z is 0 attributed to the low-contact angle droplet ($h/R < 1$, where h is height of the droplet). By rapid solvation at the air-droplet interface, the volatile vapor concentration at the droplet interface was assumed to be the same as the concentration in the air [28]. The concentration profile along with the droplet interface can be estimated as the volatile vapor concentration as,

$$\Delta c_{droplet} = c_0 r_0 \left(\frac{1}{d} - \frac{1}{\sqrt{(d+R)^2 + R^2}} \right) \quad (2)$$

where we assumed that the surface tension varied linearly in the low mass fraction regime under the 5% mass fraction [12, 29].

With heating of the volatile liquid, modified vapor concentration ($c_{0,modified}$) as a function of temperature can be theoretically estimated from Dalton’s law and the Antoine equation as,

$$c_{0,modified}(T) = \frac{P_{vap}}{P_{atm}} \times \frac{M}{V_{mol}} = \left[10^{A-B/(C+T)} / P_{atm} \right] \times \frac{M}{V_{mol}} \quad (3)$$

where P_{vap} is the vapor pressure which is estimated from $10^{A-B/(C+T)}$, where A , B , and C are component-specific constants of the Antoine equation [3, 30]. P_{atm} is the atmosphere pressure, M is molecular weight of substance, and V_{mol} is molar volume. For volatile liquids (ethanol, acetone, and IPA) used in this study, the three constants of the Antoine equation are summarized with their molecular weight in **Table 1** [30–32]. The local surface tension difference is consequently estimated as [3],

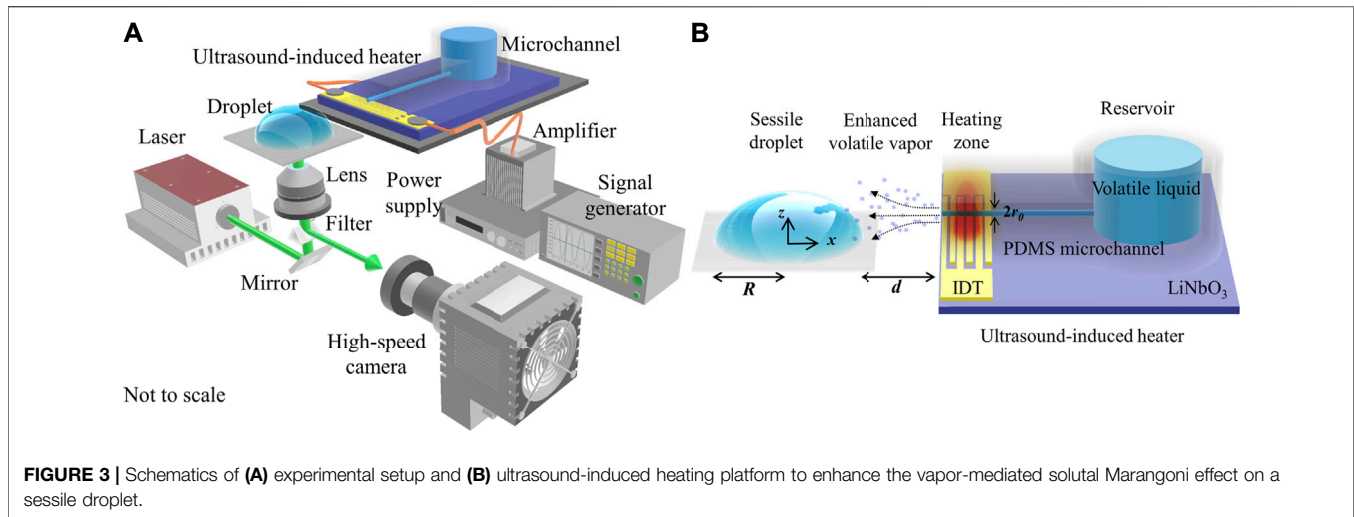
$$\Delta \gamma = \beta \Delta c_{droplet} = \beta c_{0,modified}(T) r_0 \left(\frac{1}{d} - \frac{1}{\sqrt{(d+R)^2 + R^2}} \right) \quad (4)$$

where β is the proportionality constant of the volatile liquids available in the literature [29, 33]. From this theoretical estimation, we can hypothesize that the surface tension gradient is proportional to the temperature-dependent $c_{0,modified}$ of the volatile liquid and that the vapor-mediated solutal Marangoni flows can be controlled by the UIH.

Figure 2B indicates the initial vapor concentration at the microchannel ($c_{0,modified}$) as a function of the temperature (T) for three volatile liquids used in this study (acetone, IPA, and ethanol). The theoretical calculation demonstrates that the volatile vapor concentration increases with temperature. Since the increased local vapor concentration is closely related to the increase in the local surface tension gradient along the droplet interface, the vapor-mediated solutal Marangoni flows can be significantly enhanced in the proposed method. For experimental validation, **Figure 2C** shows the stacked image of 1 μm -diameter particle-laden droplets exposed to the 50°C acetone vapor at the right-most end of the droplet, where symmetrical Marangoni vertical flows can be clearly observed, as predicted. A detailed discussion on the quantitative experimental flow investigation will be provided in the subsequent section.

EXPERIMENTAL

Figure 3A shows a schematic of the experimental setup of the present study. A $2 \pm 0.2 \mu\text{L}$ sessile drop on a glass coverslip was placed on an inverted fluorescent microscope (IX-73, Olympus) equipped with a 4× objective lens (UPlanFL N 4×, Olympus) with the UIH device where a volatile liquid is stored in a reservoir. As the UIH is applied to the volatile liquid, the vaporized volatile liquid induces a local surface tension gradient of the sessile droplet at room temperature of 20°C. The droplet radius was fixed as $R = 1.25 \text{ mm}$, and the distance between the droplet and the heater was varied as $d = 2\text{--}6 \text{ mm}$. As the droplet height (h) is



much smaller than the droplet radius (R), such that $h/R < 1$, the flow confined within the low-aspect ratio droplets can be approximated as a 2D flow [3]. The dynamic viscosity of the liquid drop was varied $\mu = 1.00\text{--}6.00\text{ mPa}\cdot\text{s}$ using water-glycerol mixture solution with varying ratios. The IDT in the ultrasound-induced heater was actuated by an amplified sinusoidal AC signal produced by a signal generator (N931A, Keysight), an amplifier (ZHL-100W-GAN+, Mini-Circuits), and a power supply (EX50-24, ODA technology). For quantitative investigation of the enhanced solutal Marangoni flows, we apply particle image velocimetry (PIV) with a high-speed camera (VEO710-L, Phantom) and a 532 nm laser (MGL-F-532, Changchun New Industries Optoelectronics Technology) and fluorescence filter for 460–495 nm. As tracing particles for the in-droplet flows, 1 wt % of the 1 μm -diameter red fluorescent polymer particles (Duke Scientific) suspended in DI water was used. The particle images were captured at 300–1,300 fps when the internal droplet flow was under steady-state conditions (approximately 2–3 s after the onset of evaporation). Due to a low aspect ratio of height to diameter of the sessile droplets, we assumed that the two-dimensional flow was dominant within the sessile droplets; therefore, the focal plane for the particle images was set to be just above the glass coverslip where the in-plane 2D Marangoni flow was dominant. The flow velocity was calculated by the 2D cross-correlation using an interrogation window of $128 \times 128\text{ pixels}^2$ with 50% overlap for a coarse grid and $68 \times 68\text{ pixels}^2$ with 50% overlap for a refined grid system by utilizing PIVlab [34, 35]. For the PIV experiments, the Stokes number ($St = \tau_p/\tau_f$) was approximately calculated as $St \approx 9.3 \times 10^{-7}$ where $\tau_p = (1/18)\rho_p d_p^2/\mu_f$ is the particle response time, $\tau_f = R/V$ is the flow time scale, ρ_p is the density of the particles, d_p is the particle diameter, μ_f is the dynamic viscosity of the fluid, and V is the flow velocity obtained from the PIV results. For quantification of the mixing, we captured images using a DSLR camera (Canon 850D, Canon) with a macro lens (Canon EF-S 60 mm f2.8 Macro USM, Canon). From the captured images, we converted the images to 8-bit greyscale images and extracted grey-values by using the ImageJ software (<http://rsb.info.nih.gov/ij/>).

As shown in **Figure 3B**, the temperature of the volatile liquid in the microchannel was controlled by the improved UIH method. The PDMS microchannel with a radius (r_0) of 0.5 mm was fabricated by a 3D printed mold. The multilayer of the AgNW-embedded thin PDMS membranes was placed beneath the PDMS microchannel block and was used to absorb ultrasound for energy-efficient UIH. The multilayered AgNW-PDMS composite was fabricated by the following steps. First, a thin PDMS membrane with 40 μm thickness was fabricated by spin-coating of uncured PDMS precursor solution (degassed Sylgard 184 elastomer and curing agent mixture at 10:1 ratio). After thermal-curing of the single membrane at 65°C for 2 h, oxygen plasma treatment (Covance, Femto Science) was applied on the membrane to increase the surface energy. The $43 \pm 5\text{ nm}$ -diameter, $19 \pm 5\text{ }\mu\text{m}$ -long AgNWs suspended in IPA were deposited on the membrane on the plasma-treated thin PDMS membrane by air-brushing, and this process was repeated five times to construct a multilayered AgNW-PDMS composite. A pair of Cr and Au bimetallic electrodes with thickness of 20 and 100 nm was deposited by photolithography, e-beam evaporation, and lift-off process on a 500 μm thick, 128°-rotated Y-cut X-propagating LiNbO₃ wafer (MTI Korea). The IDT has a total aperture of 2.9 mm, electrode spacing is $\lambda/4 = 32.5\text{ }\mu\text{m}$ where λ is the acoustic wavelength, and a finger pair number of $N = 20$. The scattering parameter (S_{11}) was measured to identify the resonant frequency of the IDT $f = 29\text{ MHz}$ using a vector network analyzer (E5071B, Agilent Technologies), and the actual electric power applied to the IDT was measured by an oscilloscope (MSO8104A, Agilent Technologies).

RESULTS AND DISCUSSION

Heating-Mediated Enhanced Solutal Marangoni Effect

We conducted quantitative analysis on the heating-mediated enhanced solutal Marangoni effect through theoretical and experimental investigation with PIV. **Figure 4** shows the 2D

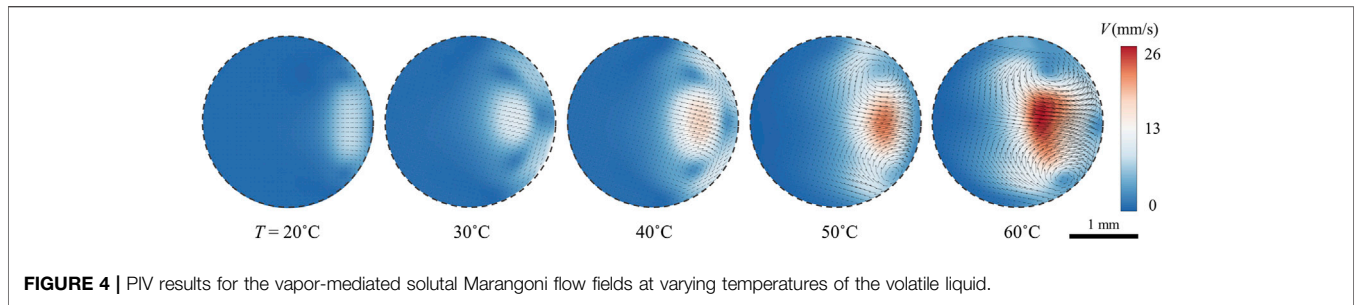


FIGURE 4 | PIV results for the vapor-mediated solutal Marangoni flow fields at varying temperatures of the volatile liquid.

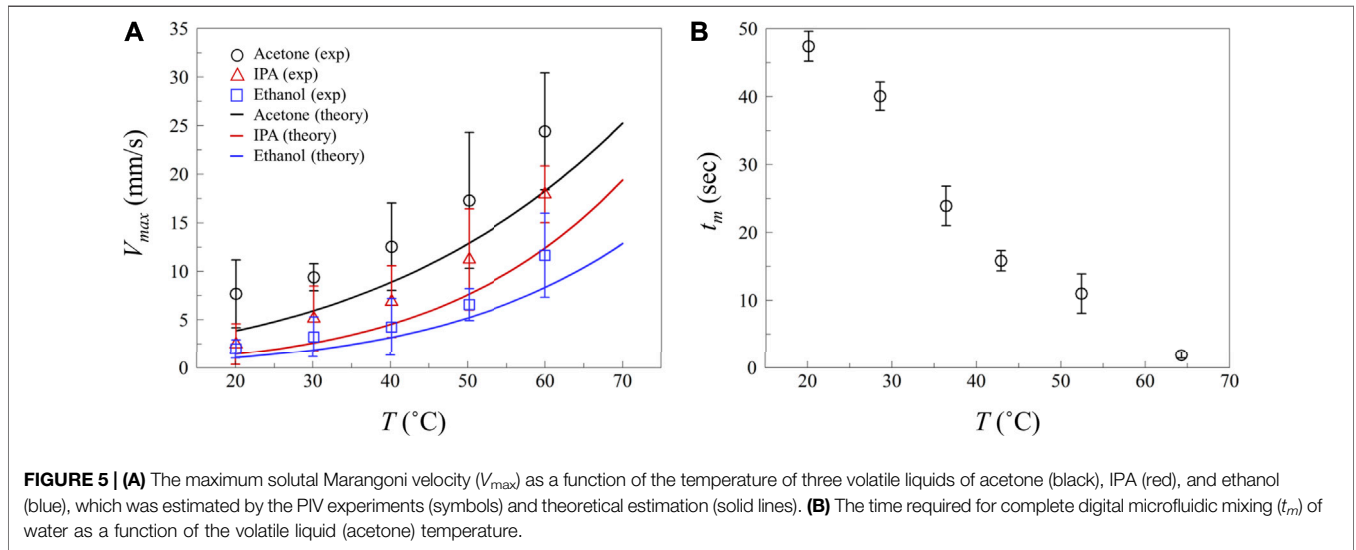


FIGURE 5 | **(A)** The maximum solutal Marangoni velocity (V_{max}) as a function of the temperature of three volatile liquids of acetone (black), IPA (red), and ethanol (blue), which was estimated by the PIV experiments (symbols) and theoretical estimation (solid lines). **(B)** The time required for complete digital microfluidic mixing (t_m) of water as a function of the volatile liquid (acetone) temperature.

velocity fields of the $2 \pm 0.2 \mu\text{L}$ sessile drop of water/glycerol solution ($R = 1.25 \text{ mm}$, $h = 0.625 \text{ mm}$, and $\mu = 1.98 \text{ mPa s}$) locally exposed to vaporized acetone at varying temperature $T = 20\text{--}60^\circ\text{C}$ with the distance $d = 2 \text{ mm}$. The acetone temperature in the 0.5 mm radius microchannel was controlled by UIH. A pair of the solutal Marangoni vortices was observed in all cases, and the solutal Marangoni flow velocity was measured to increase as the temperature of the volatile liquid increased. It was attributed that the increased vapor concentration induced by the increased temperature of the volatile liquid led to the enhanced vapor-mediated solutal Marangoni effect driven by increased local surface tension gradient along the droplet interface.

At a low Reynolds number ($Re < 1$), the Marangoni force per unit volume is mainly balanced by the viscous force per unit volume in the sessile droplet. The solutal Marangoni flow velocity can be theoretically estimated as [3],

$$V \approx \frac{\Delta\gamma h}{\mu R} = \frac{\beta c_{0,modified} r_0 h}{\mu R} \left(\frac{1}{d} - \frac{1}{\sqrt{(d+R)^2 + R^2}} \right) \quad (5)$$

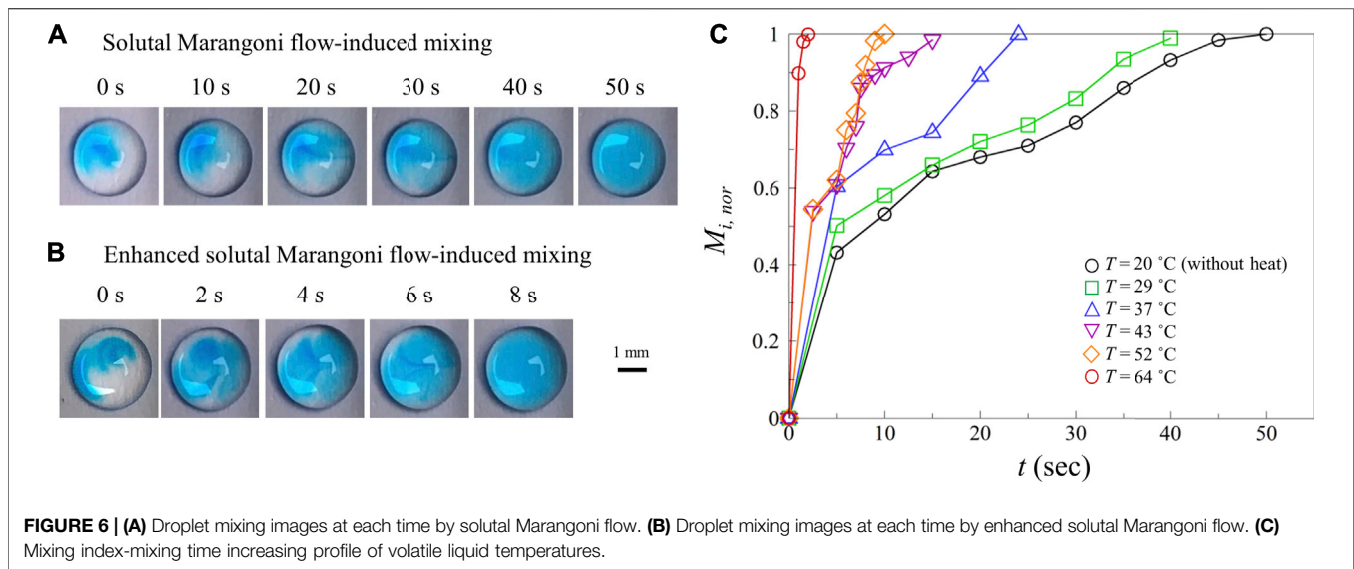
For investigation on the volatile liquid temperature effect on the solutal Marangoni effect, we performed five repeated experiments at varying volatile liquid temperatures of $T = 20, 30, 40, 50,$ and 60°C for acetone, IPA, and ethanol as volatile liquids for water sessile droplets, while all other parameters ($R, h, d, r_0,$ and μ) remained the

same. **Figure 5A** shows the maximum solutal Marangoni velocity (V_{max}) as a function of the temperature of three volatile liquids of acetone (black), IPA (red), and ethanol (blue), which was estimated by the PIV experiments (symbols) and theoretical estimation (solid lines). The error bar represents the standard deviation of the measured values from the repeated experiments. The theoretical estimation was conducted by applying the experimental conditions. Despite the discrepancy between the experimental and theoretical values for V_{max} , the maximum Marangoni flow velocity was confirmed to monotonically increase by accelerating the vaporization of the volatile liquid with increasing temperature in both all cases. The theoretically estimated V_{max} slightly deviated from the measured V_{max} from the PIV experiments can be attributed to the linear surface tension profile assumption, inaccurate measurement of the experimental conditions, and 3D Marangoni vortical flow structure [3, 12, 29].

For quantification of the droplet mixing, we introduced a mixing index defined as [36],

$$M_i = \frac{1}{C''} \sqrt{\frac{\sum (C_j - C_c)^2}{N}} \quad (6)$$

where C'' is the mean grey value for the unmixed condition, C_c is the mean grey value for the completely mixed condition, C_j is the grey value in each pixel, and N is the total number of pixels. The normalized mixing index to indicate the index ranging



from 0 (unmixed) to 1 (completely mixed) was then expressed as,

$$M_{i,nor} = 1 - \frac{M_i - M_f}{M_0 - M_f} \quad (7)$$

where M_0 is the mixing index for the initial unmixed case and M_f is the mixing index for the completely mixed case. **Figure 5B** shows the time (t_m) required for complete droplet mixing of pure DI water ($\mu = 1.00$ mPa s) in which $M_{i,nor} = 1$, driven by the vapor-mediated solutal Marangoni effect at varying the acetone temperature at $T = 20$ – 64°C . We used the erioglucine disodium salt solution in DI water for visualization of the droplet mixing. As shown in **Figure 5B**, the time required for complete droplet mixing is significantly reduced with increasing temperature of the acetone. Especially at $T = 60^\circ\text{C}$ above the acetone boiling temperature, immediate droplet mixing was observed within a second whereas the solutal Marangoni flow-based mixing at room temperature of $T = 20^\circ\text{C}$ required more than 47 s for complete mixing. The error bar represents the standard deviation of the measured t_m from the ten repeated experiments, mainly due to somewhat inconsistent injecting location of the dye solution on the sessile droplets.

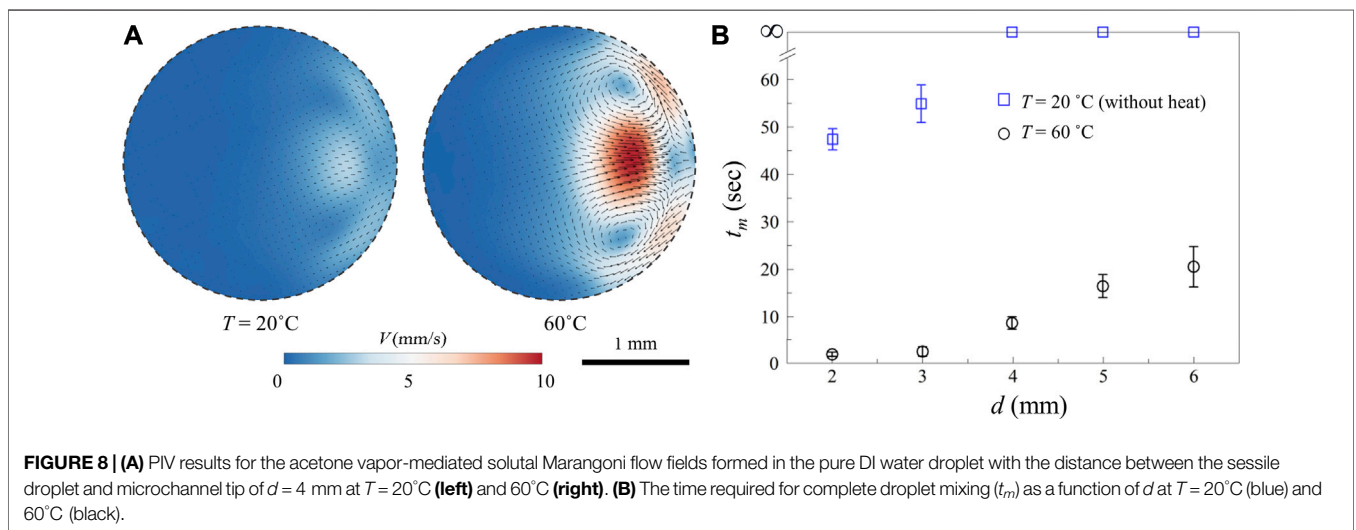
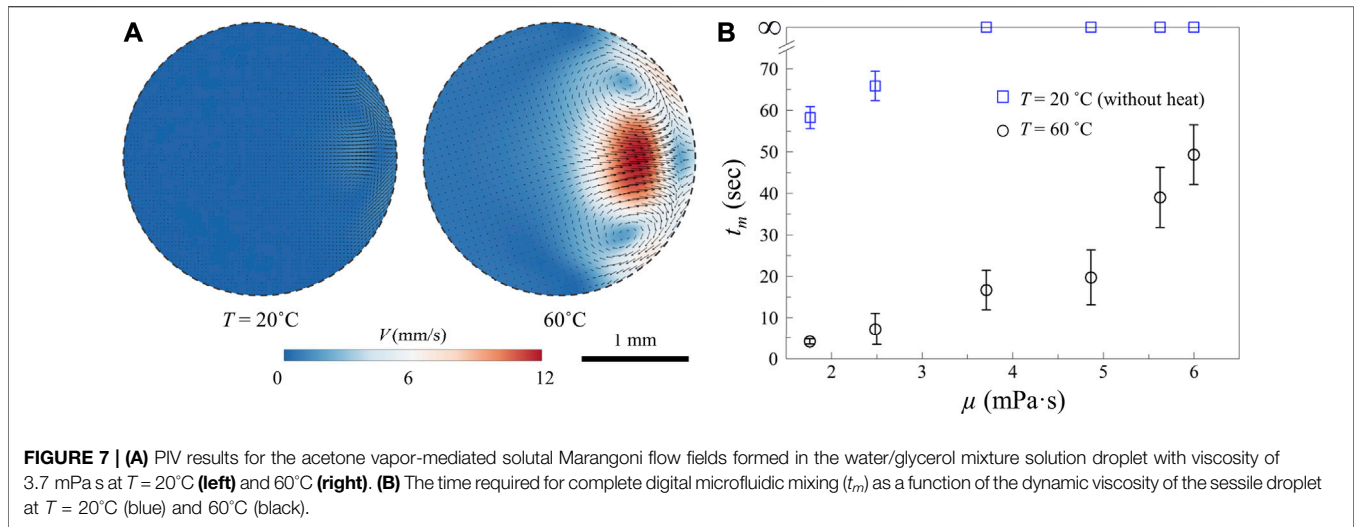
The time-sequential bright-field images of the droplet mixing of the pure DI water and erioglucine disodium salt solution in DI water by acetone-mediated solutal Marangoni flow-induced mixing at room temperature (**Figure 6A**) and at $T = 52^\circ\text{C}$ (**Figure 6B**) were presented. As clearly shown in the figures, the heating-mediated solutal Marangoni flows can significantly enhance the digital microfluidic mixing efficiency. **Figure 6C** represents the normalized mixing index as a function of time for varying temperatures of $T = 20$ – 64°C . In accordance with the theoretical model and experimental data shown in **Figure 6B**, the time rate of change of the normalized mixing index increased with increasing acetone temperature. From the experiments, we confirmed that the heating-mediated increase in the local

vaporized volatile liquid concentration induced enhanced solutal Marangoni effect for rapid digital microfluidic mixing of sessile droplets.

Viscosity and Distance Effects on Solutal Marangoni Flow

As in Eq. 5, the vapor-mediated solutal Marangoni flow velocity is inversely proportional to the dynamic viscosity of the droplet liquid. As the droplet viscosity is increased, the contribution of the viscous dissipation becomes significant, thereby disturbing the volatile vapor-mediated Marangoni flows formed inside the sessile droplets. **Figure 7A** shows the 2D velocity fields of the 2 ± 0.2 μL sessile droplet of water/glycerol solution ($R = 1.25$ mm, $h = 0.625$ mm, and $\mu = 3.7$ mPa s) locally exposed to vaporized acetone at $T = 20^\circ\text{C}$ (left) and 60°C (right) with the distance $d = 2$ mm. As predicted from the theoretical estimation, the conventional vapor-mediated solutal Marangoni flow-induced mixing method cannot be utilized for the viscous liquid droplets, causing the application of the passive method to be strictly limited to the low-viscosity liquid drop mixing. On the other hand, the heating-mediated enhanced solutal Marangoni flow at $T = 60^\circ\text{C}$ can induce the Marangoni flow velocity of higher than 10 mm/s, which was enough to mix the viscous liquid droplets. Various liquids used in sessile droplet-based microfluidics have higher dynamic viscosity such as blood with $\mu \sim 3.5$ mPa s [37].

For further quantitative analysis, we performed the repeated experiments with varying the dynamic viscosity of $\mu = 1.78$ – 6.00 mPa s by changing the mixing ratio of the water and glycerol mixture solution [38, 39], as shown in **Figure 7B**. The solutal Marangoni flow without heating (blue) at room temperature of 20°C , the droplet mixing can be achieved for low-viscosity droplets with $\mu < 2.5$ mPa s. However, this passive method required a comparably long time of approximately 1 min for the complete mixing with $M_{i,nor} = 1$ to be used for practical



application. Further, for high-viscosity liquid droplets with $\mu > 3.5$ mPa s, the droplet mixing was not achievable by the room-temperature solutal Marangoni effect. On the contrary, the heating-mediated enhanced solutal Marangoni flow can be applied to rapid mixing with $t_m < 10$ s for low-viscosity droplets with $\mu < 2.5$ mPa s. Even for high-viscosity droplets with $\mu > 3.5$ mPa s, the enhanced solutal Marangoni flow-induced droplet mixing was clearly observed with a relatively increased time required for complete mixing. These results demonstrate the proposed active Marangoni flow-based droplet mixing method outperforms the previous passive method in terms of improved applicability for various kinds of liquids.

As discussed in the theoretical modeling (Eqs. 2, 4, 5), the distance between the sessile droplet and microchannel tip (d) also plays an important role in the vapor-mediated solutal Marangoni flow. Since the vapor concentration profile, surface tension gradient, and the solutal Marangoni flow velocity are heavily dependent on d , we conducted droplet mixing experiments with varying $d = 2\text{--}6$ mm. **Figure 8A** shows the 2D Marangoni flow

velocity fields of the 2 ± 0.2 μL sessile droplet of pure DI water ($R = 1.25$ mm, $h = 0.625$ mm, and $\mu = 1.0$ mPa s) locally exposed to vaporized acetone at $T = 20^\circ\text{C}$ (left) and 60°C (right) with the distance $d = 4$ mm. From the theoretical model (Eqs. 2, 4, 5), we could predict that volatile vapor concentration would be decreased as increasing distance d so that the flow velocity also would decrease, leading to increased requiring time for complete droplet mixing. At room temperature, the acetone vapor-mediated solutal Marangoni effect was observed to be negligible, and the droplet mixing was not achieved. On the other hand, at an increased temperature of $T = 60^\circ\text{C}$ by UIH, the acetone vapor-mediated solutal Marangoni flow velocity was measured to exceed 10 mm/s, and the complete droplet mixing was achieved within 10 s.

Figure 8B shows the time required for complete droplet mixing (t_m) with varying $d = 2, 3, 4, 5,$ and 6 mm at $T = 20^\circ\text{C}$ (blue) without heating and 60°C (black) by UIH. In compliance with the theoretical prediction, the droplet mixing time required for $M_{i,nor} = 1$ increased with increasing d in all cases. For the

conditions with $d \leq 3$ mm, room-temperature solutal Marangoni effect could be applicable for droplet mixing with $t_m < 1$ min; however, the droplet mixing cannot be achieved when the sessile droplet was placed far from the volatile liquid with $d \geq 4$ mm, the droplet mixing cannot be achieved by the passive solutal Marangoni effect. On the other hand, at increased acetone temperature of $T = 60^\circ\text{C}$ with the help of the UIH method, the enhanced solutal Marangoni effect enabled rapid droplet mixing with $t_m < 3$ s for $d \leq 3$ mm. Even with $d \geq 4$ mm, the droplet mixing was achieved with $t_m < 20$ s by the heating-mediated solutal Marangoni effect, which was impossible in the passive method. These results imply that the enhanced solutal Marangoni flow-based mixing method can operate under less strict conditions for the location of the sessile droplets and the volatile liquid vaporization, preventing potential direct contact of the liquids for cross-contamination and improving the stability of the working conditions.

CONCLUSION

We have improved the energy efficiency of the UIH by introducing a nature-inspired fibrous network-embedded ultrasound absorbing layer to enhance the ultrasound absorption based on the microscale hairy structure on the moth wing [18, 19, 21, 23]. By the infrared thermal imaging of the increased temperature by UIH, we found a 61.09% improvement in the temperature increase under the same electrical power applied to the heater. The improved UIH method was applied to enhance vapor-mediated solutal Marangoni effect for digital microfluidic mixing. The increased temperature accelerated the vaporization of the volatile liquid, and the local surface tension gradient was increased accordingly, resulting in the enhanced solutal Marangoni flow. We conducted theoretical investigation on the enhanced solutal Marangoni flow based on the steady-state Poisson equation, Dalton's law, and Antoine equation to estimate the enhanced solutal Marangoni flow velocity [3, 12, 28, 29, 31]. We also performed the PIV experiments for experimental validation and found that the

theoretical estimation and the measured values were in good agreement for varying volatile liquid temperatures. For analysis on the droplet viscosity and distance effects on the solutal Marangoni effects, we measured the time required for complete mixing under various conditions. From the experimental results, we confirmed that the enhanced solutal Marangoni flow-based mixing can improve the droplet mixing performance with reduced mixing time and mixing abilities even for high-viscosity liquid droplets and far-placed droplets from the volatile liquid, improving the practical applicability. Therefore, we expect that the proposed enhanced solutal Marangoni effect with the improved UIH can offer new perspectives to digital droplet microfluidic mixing in various fields including biochemical assays, clinical diagnostics, and drug screening.

DATA AVAILABILITY STATEMENT

The raw data supporting the conclusion of this article will be made available by the authors, without undue reservation.

AUTHOR CONTRIBUTIONS

JP conceived and supervised the research. BC and WK designed and performed the experiments. BC, WK, GY, and HJ analyzed the experimental results. All authors contributed to the writing of the manuscript and have given approval to the final version of the manuscript.

FUNDING

This work was supported by the National Research Foundation of Korea (NRF) grants funded by the Korea government (MSIT) (Nos. 2020R1A5A8018367 and 2020R1F1A1048611) and Nanomedical Devices Development Project of NNFC (CSM2101M001).

REFERENCES

- Whitesides GM. The Origins and the Future of Microfluidics. *Nature* (2006) 442(7101):368–73. doi:10.1038/nature05058
- Ho C-M, and Tai Y-C. MICRO-ELECTRO-MECHANICAL-SYSTEMS (MEMS) AND FLUID FLOWS. *Annu Rev Fluid Mech* (1998) 30(1): 579–612. doi:10.1146/annurev.fluid.30.1.579
- Park J, Ryu J, Sung HJ, and Kim H. Control of Solutal Marangoni-Driven Vortical Flows and Enhancement of Mixing Efficiency. *J Colloid Interf Sci* (2020) 561:408–15. doi:10.1016/j.jcis.2019.11.006
- Jakeway SC, de Mello AJ, and Russell EL. Miniaturized Total Analysis Systems for Biological Analysis. *Fresenius' J Anal Chem* (2000) 366(6):525–39. doi:10.1007/s002160051548
- Pollack MG, Fair RB, and Shenderov AD. Electrowetting-based Actuation of Liquid Droplets for Microfluidic Applications. *Appl Phys Lett* (2000) 77(11): 1725–6. doi:10.1063/1.1308534
- Samiei E, and Hoorfar M. Systematic Analysis of Geometrical Based Unequal Droplet Splitting in Digital Microfluidics. *J Micromech Microeng* (2015) 25(5): 055008. doi:10.1088/0960-1317/25/5/055008
- Samiei E, de Leon Derby MD, den Berg AV, and Hoorfar M. An Electrohydrodynamic Technique for Rapid Mixing in Stationary Droplets on Digital Microfluidic Platforms. *Lab Chip* (2017) 17(2):227–34. doi:10.1039/C6LC00997B
- Mugele F, and Baret J-C. Electrowetting: from Basics to Applications. *J Phys Condens Matter* (2005) 17(28):R705–R774. doi:10.1088/0953-8984/17/28/r01
- Hessel V, Löwe H, and Schönfeld F. Micromixers—a Review on Passive and Active Mixing Principles. *Chem Eng Sci* (2005) 60(8):2479–501. doi:10.1016/j.ces.2004.11.033
- Beebe DJ, Mensing GA, Walker GM, and Walker GM. Physics and Applications of Microfluidics in Biology. *Annu Rev Biomed Eng* (2002) 4(1):261–86. doi:10.1146/annurev.bioeng.4.1.261
- Lee JH, Lee KH, Won JM, Rhee K, and Chung SK. Mobile Oscillating Bubble Actuated by AC-Electrowetting-On-Dielectric (EWOD) for Microfluidic Mixing Enhancement. *Sensors Actuators A: Phys* (2012) 182:153–62. doi:10.1016/j.sna.2012.05.022

12. Malinowski R, Volpe G, Parkin IP, and Volpe G. Dynamic Control of Particle Deposition in Evaporating Droplets by an External Point Source of Vapor. *J Phys Chem Lett* (2018) 9(3):659–64. doi:10.1021/acs.jpcclett.7b02831
13. Hegde O, Kabi P, and Basu S. Enhancement of Mixing in a Viscous, Non-volatile Droplet Using a Contact-free Vapor-Mediated Interaction. *Phys Chem Chem Phys* (2020) 22(26):14570–8. doi:10.1039/D0CP01004A
14. Kim H, Muller K, Shardt O, Afkhami S, and Stone HA. Solutal Marangoni Flows of Miscible Liquids Drive Transport without Surface Contamination. *Nat Phys* (2017) 13(11):1105–10. doi:10.1038/nphys4214
15. Ryu J, Kim J, Park J, and Kim H. Analysis of Vapor-Driven Solutal Marangoni Flows inside a Sessile Droplet. *Int J Heat Mass Transfer* (2021) 164:120499. doi:10.1016/j.ijheatmasstransfer.2020.120499
16. Lee KY, Park S, Lee YR, and Chung SK. Magnetic Droplet Microfluidic System Incorporated with Acoustic Excitation for Mixing Enhancement. *Sensors Actuators A: Phys* (2016) 243:59–65. doi:10.1016/j.sna.2016.03.009
17. T Won, KY Lee, and SK Chung eds. Acoustic Bubble Induced Microstreaming for the Enhancement of Droplet Mixing in Electrowetting (EW) Microfluidic Platforms. In: 2019 20th International Conference on Solid-State Sensors; 2019 Jun 23–27. XXXIII. Berlin, Germany: Estrel Hotel & Congress Center, Actuators and Microsystems & Euroensors (2019).
18. Ha BH, Lee KS, Destgeer G, Park J, Choung JS, Jung JH, et al. Acoustothermal Heating of Polydimethylsiloxane Microfluidic System. *Sci Rep* (2015) 5(1):11851. doi:10.1038/srep11851
19. Park J, Jung JH, Destgeer G, Ahmed H, Park K, and Sung HJ. Acoustothermal Tweezer for Droplet Sorting in a Disposable Microfluidic Chip. *Lab Chip* (2017) 17(6):1031–40. doi:10.1039/C6LC01405D
20. Lakes R, and Lakes RS. *Viscoelastic Materials*. Cambridge University Press (2009).
21. Park J, Ha BH, Destgeer G, Jung JH, and Sung HJ. Spatiotemporally Controllable Acoustothermal Heating and its Application to Disposable Thermochromic Displays. *RSC Adv* (2016) 6(40):33937–44. doi:10.1039/C6RA04075F
22. Ha BH, Park J, Destgeer G, Jung JH, and Sung HJ. Generation of Dynamic Free-form Temperature Gradients in a Disposable Microchip. *Anal Chem* (2015) 87(22):11568–74. doi:10.1021/acs.analchem.5b03457
23. Neil TR, Shen Z, Robert D, Drinkwater BW, and Holderied MW. Moth Wings Are Acoustic Metamaterials. *Proc Natl Acad Sci USA* (2020) 117(49):31134–41. doi:10.1073/pnas.2014531117
24. Iasella SV, Sun N, Zhang X, Corcoran TE, Garoff S, Przybycien TM, et al. Flow Regime Transitions and Effects on Solute Transport in Surfactant-Driven Marangoni Flows. *J Colloid Interf Sci* (2019) 553:136–47. doi:10.1016/j.jcis.2019.06.016
25. Cira NJ, Benusiglio A, and Prakash M. Vapour-mediated Sensing and Motility in Two-Component Droplets. *Nature* (2015) 519(7544):446–50. doi:10.1038/nature14272
26. Sadafi H, Dehaeck S, Rednikov A, and Colinet P. Vapor-mediated versus Substrate-Mediated Interactions between Volatile Droplets. *Langmuir* (2019) 35(21):7060–5. doi:10.1021/acs.langmuir.9b00522
27. Kabi P, Pal R, and Basu S. Moses Effect: Splitting a Sessile Droplet Using a Vapor-Mediated Marangoni Effect Leading to Designer Surface Patterns. *Langmuir* (2020) 36(5):1279–87. doi:10.1021/acs.langmuir.9b03690
28. Wilson MA, and Pohorille A. Adsorption and Solvation of Ethanol at the Water Liquid–Vapor Interface: A Molecular Dynamics Study. *J Phys Chem B* (1997) 101(16):3130–5. doi:10.1021/jp962629n
29. Vazquez G, Alvarez E, and Navaza JM. Surface Tension of Alcohol Water + Water from 20 to 50 .Degree.C. *J Chem Eng Data* (1995) 40(3):611–4. doi:10.1021/je00019a016
30. Rodgers RC, and Hill GE. EQUATIONS FOR VAPOUR PRESSURE VERSUS TEMPERATURE: DERIVATION AND USE OF THE ANTOINE EQUATION ON A HAND-HELD PROGRAMMABLE CALCULATOR. *Br J Anaesth* (1978) 50(5):415–24. doi:10.1093/bja/50.5.415
31. Thomson GW. The Antoine Equation for Vapor-Pressure Data. *Chem Rev* (1946) 38(1):1–39. doi:10.1021/cr60119a001
32. Biddiscombe DP, Collerson RR, Handley R, Herington EFG, Martin JF, and Sprake CHS. 364. Thermodynamic Properties of Organic Oxygen Compounds. Part VIII. Purification and Vapour Pressures of the Propyl and Butyl Alcohols. *J Chem Soc* (1963)(0) 1954–7. doi:10.1039/JR9630001954
33. Howard KS, and McAllister RA. Surface Tension of Acetone-Water Solutions up to Their normal Boiling Points. *Aiche J* (1957) 3(3):325–9. doi:10.1002/aic.690030308
34. Adrian L, Adrian RJ, and Westerweel J. *Particle Image Velocimetry*. Cambridge University Press (2011).
35. Thielicke W, and Stamhuis E. PIVlab—Towards User-Friendly, Affordable and Accurate Digital Particle Image Velocimetry in MATLAB. *J open Res Softw* (2014) 2(1). doi:10.5334/jors.bl
36. Niu X, Liu L, Wen W, and Sheng P. Active Microfluidic Mixer Chip. *Appl Phys Lett* (2006) 88(15):153508. doi:10.1063/1.2195567
37. Anastasiou AD, Spyrogianni AS, Koskinas KC, Giannoglou GD, and Paras SV. Experimental Investigation of the Flow of a Blood Analogue Fluid in a Replica of a Bifurcated Small Artery. *Med Eng Phys* (2012) 34(2):211–8. doi:10.1016/j.medengphy.2011.07.012
38. Cheng N-S. Formula for the Viscosity of a Glycerol–Water Mixture. *Ind Eng Chem Res* (2008) 47(9):3285–8. doi:10.1021/ie071349z
39. Segur JB, and Oberstar HE. Viscosity of Glycerol and its Aqueous Solutions. *Ind Eng Chem* (1951) 43(9):2117–20. doi:10.1021/ie50501a040

Conflict of Interest: The authors declare that the research was conducted in the absence of any commercial or financial relationships that could be construed as a potential conflict of interest.

Publisher's Note: All claims expressed in this article are solely those of the authors and do not necessarily represent those of their affiliated organizations, or those of the publisher, the editors and the reviewers. Any product that may be evaluated in this article, or claim that may be made by its manufacturer, is not guaranteed or endorsed by the publisher.

Copyright © 2021 Cha, Kim, Yoon, Jeon and Park. This is an open-access article distributed under the terms of the Creative Commons Attribution License (CC BY). The use, distribution or reproduction in other forums is permitted, provided the original author(s) and the copyright owner(s) are credited and that the original publication in this journal is cited, in accordance with accepted academic practice. No use, distribution or reproduction is permitted which does not comply with these terms.